J Appl Electrochem (2012) 42:833–841
DOI 10.1007/s10800-012-0446-9

ORIGINAL PAPER

Direct conversion of dimethyl ether in high-temperature polymer electrolyte fuel cells under stationary and dynamic conditions

Christoph Noack · Josef Kallo · Andreas K. Friedrich

Received: 4 May 2012 / Accepted: 3 July 2012 / Published online: 18 July 2012
© Springer Science+Business Media B.V. 2012

Abstract The behavior of a polybenzimidazole-based high-temperature polymer electrolyte membrane fuel cell using dimethyl ether (DME) as fuel was investigated under stationary and dynamic load conditions. The power density was enhanced significantly with an increase of both operating temperature and anodic water stoichiometry. Likewise, the power density decreased with increasing DME stoichiometry. The characterization of the dynamic operation showed a strong qualitative similarity to low-temperature direct methanol fuel cells. The development of the cell voltage after a spontaneous change of cell current density could be assigned to the electrochemical oxidation of an intermediate species.

Keywords Fuel cell · High-temperature PEM · Dimethyl ether · Steady state and dynamic operation

1 Introduction

Worldwide, researchers are looking for ways to replace the prevailing conventional power generation with alternative, resource-saving, and low-polluting alternatives. However, it is widely recognized that in the medium term there will be no optimal solution matching all requirements. In the probable rather complex energy-generation scenario, fuel cells will play an important role specifically for clean power generation. With its high efficiency and high power density, this technology is able to meet the requirements of many small- and medium-sized power generation applications.

C. Noack (✉) · J. Kallo · A. K. Friedrich
German Aerospace Center (DLR), 70569 Stuttgart, Germany
e-mail: christoph.noack@dlr.de

Hydrogen is the cleanest fuel, especially when it is produced in a sustainable way. However, the serious disadvantage of hydrogen is the lack of applicable space- and weight-efficient possibilities for storage and transportation. An alternative to hydrogen could be hydrogen-rich hydrocarbons. Methanol, for example, is a well-studied fuel for use in direct fuel cells, even at elevated temperatures in a gaseous state [1]. Together, the high energy density of a liquid fuel, the possibility of industrial production in large amounts, and liquid transportation could compensate for the lower power densities of liquid fuels compared to hydrogen-fueled fuel cells. But even methanol has disadvantages, mainly because of its high toxicity and high crossover rate in Nafion®-based low-temperature direct methanol fuel cells (LT-DMFC) [2].

Therefore, in the search for an alternative, hydrogen-rich hydrocarbons as fuel are of great interest. One promising option could be dimethyl ether (DME). Despite the fact that DME requires three times more water for the anodic reaction compared to a DMFC (Eq. 1), the required energy for the evaporation of fuel and water in relation to the yield of protons is about 10 % less. From a systems point of view, it is advantageous that the boiling point of DME under atmospheric pressure is about −25 °C. Therefore, at room temperature, DME can be stored as liquid at low pressures (4–5 bar) but it becomes gaseous at atmospheric pressures. There is no need to heat it up to provide a gaseous feeding of the cell. Further, DME has only an ethereal effect but it is not potentially lethal like methanol. DME is also interesting in that it can be produced and delivered in high quantities, as is the case with common fuel, e.g., in China. In case of the accidental escape of DME into the air, it decomposes within a couple of hours and therefore cannot be seen as dangerous for the ozone layer [3]. Additional properties are discussed in detail in [4] and [5].

However, despite the above-mentioned advantages, recently demonstrated direct DME fuel cells (DDFC) exhibited a rather low power density due to sluggish kinetics and the large activation energies required for water dissociation [6, 7].

Nafion®-based low-temperature polymer electrolyte membrane fuel cells (LT-PEMFC) do not necessarily need a gaseous fuel supply. However, they do need highly humidified gas to enable water-based proton transport through the membrane. This implies additional system complexity and may lead to a reduction of system efficiency. Polybenzimidazole (PBI)-based high-temperature polymer electrolyte membrane fuel cells (HT-PEMFC) do not need water to ensure proton conductivity because the protons are carried by the phosphoric acid with which the PBI is doped. This reduces system complexity and weight. In addition, the operating temperature of a HT-PEMFC is 130–180 °C. These elevated temperatures should lead to enhanced reaction kinetics at the catalysts and hence to higher cell power. This is important because, compared to methanol, DME has a lower electrochemical activity at low temperatures [7].

Literature that deals with DME-fueled HT-PEMFCs is very rare [8]. But there are some investigations of HT-DMFCs. Lobato et al. [9], Wang et al. [10], and Lin et al. [11] examined a PBI-based HT-PEMFC with methanol as fuel. Their work yielded results that were competitive with those of LT-DMFCs. In addition, Lin et al. [11] measured a methanol crossover, which was lower by one order of magnitude compared to a conventional DMFC operating at 80–90 °C.

Kéranguéven et al. [12], Zhang et al. [13], and Müller et al. [14] simultaneously reported that carbon monoxide (CO) was a stable intermediate of the anodic DME oxidation reaction for an LT-PEMFC. HT-PEMFCs showed only slight performance degradation due to CO poisoning when compared to LT-PEM fuel cells. Good tolerance of a Pt/C catalyst was observed with 3 % of CO at 200 °C up to either a current density of 1.0 A cm^{-2} or a cell voltage above 0.5 V [15], and with 3 and 5 % of CO at 180 °C at moderate values of voltage [16]. It was also shown that the performance of the fuel cell operating at 210 °C was not affected by 1.0 % of CO in the anode feed [17]. These studies demonstrate that the increase of the fuel cell temperature is an alternative for diminishing the contamination of the anode catalyst, showing the viability of direct use of reformate gas on the fuel cell anode and the possibility of successful incorporation of reformers in HT-PEMFC systems. Pan et al. [18] integrated an HT-PEMFC with a methanol reformer. The CO amount at the reformate gas was below 0.2 % and at temperatures between 135 and 170 °C only a slight decrease in performance was observed in a single fuel cell.

Even if the low adsorption kinetics of DME are primarily responsible for the significant power loss of a DME-driven fuel cell [12], CO poisoning can explain at least in part the cell's behavior during stationary and dynamic operations.

The excellent performance of HT-DMFCs and their high CO tolerance motivated us to conduct measurements using a PBI-based HT-PEMFC with DME as fuel. First, experiments that show the behavior of the cell under stationary conditions and the dependence of cell performance on gas flow and temperature will be described. In the second part, the cell operated under different dynamic conditions and its behavior is described and interpreted.

2 Experiments

2.1 Setup

The test station was designed to supply the anode with a controlled flow of hydrogen, DME, and—for inertization purposes—nitrogen. On the cathode side, oxygen and air could be provided. The produced current was drawn by an electronic load (ZS506-4NVSV5, Höcherl & Hackl, Germany). The solubility of DME in liquid water is limited (1.65 M at STP [5]); therefore, it was necessary to provide a mixture of DME and water steam to the cell. A pulsation-free evaporation of controlled small amounts of water is a prerequisite for a constant power delivery, which could be reached by a so-called "pulsation-free total evaporator" (Institute of Chemical Process Engineering, University of Stuttgart, Germany). Here, water is heated up within thin capillaries, which leads to a reduction of produced bubbles.

In order to avoid possible pressure pulsations and hence effects on cell behavior by sudden temperature changes at the cell entrance, the steam-gas mixture was always heated up to cell temperature using heating cables before reaching the cell.

As the membrane electrolyte assembly (MEA) PEMEAS P1000 fuel cells from BASF (Frankfurt, Germany) were used. These fuel cells have an active area of 50 cm^2 and use 30 % Pt/Vulcan (1 mg Pt cm^{-2}) as the anode catalyst and 30 % PtNi/Vulcan (1 mg cm^{-2} alloy) as the cathode catalyst. The uncompressed electrodes have a thickness of about 400 μm and the membrane has a thickness of about 100 μm.

2.2 Methodology

One objective of the work was to determine the cell behavior under various steady-state operating conditions to develop optimal parameters for constant operation. For this purpose, polarization curves were recorded and the anodic

off-gas was measured by gas chromatography (GC). The anodic off-gas could not be analyzed because the flow rate was too low for our GC equipment. The polarization curves were measured galvanostatically for cell currents between 0 and 0.2 A cm^{-2}. Each load level was maintained for 9 min. During this time, three GC measurements were performed. In each case, the last measurement was taken for analysis.

Equation 1 shows the global anodic reaction of DME. Similar to other hydrocarbons, DME needs water for a total conversion to CO_2.

$$CH_3OCH_3 + 3H_2O \rightarrow 2CO_2 + 12H^+ + 12e^- \quad (1)$$

To see the influence of excess of water and DME, we varied the water stoichiometry between 2 and 6 and the DME stoichiometry between 2 and 12. According to Eq. 1 the water stoichiometry corresponds to the multiple of three water molecules that are required in each reaction step. All measurements were performed at 140 and 180 °C. The upper gas flow limits were set by fluctuations of cell voltage that appeared above a certain amount of water or DME. In the low current density range between 0 and 0.04 A cm^{-2}, the gas flow could not be controlled according to the corresponding stoichiometry. It was maintained at a corresponding current density of 0.04 A cm^{-2}.

In order to determine if a fuel cell/fuel combination was appropriate for a specific application, a characterization and quantification of the time-dependent development of the cell voltage under changing load conditions was necessary. We performed several sudden current density steps between 0 and 0.16 A cm^{-2}, with a constant gas flow corresponding to a cell current density of 0.16 A cm^{-2}.

3 Results and discussion

3.1 Steady state

3.1.1 Dependence on H_2O stoichiometry

First, the dependence of cell performance on water stoichiometry was investigated by recording polarization curves (Fig. 1). In comparison to PBI-based DMFCs, the performance of the cells is low [9]. However, there is a strong similarity in performance to that of high-temperature DDFCs described in [8], which were obtained using PBI-based membranes. The reason for the low performance is primarily due to high activation losses as indicated by the curve at low currents. This is in agreement with the low electro-oxidation of DME compared to methanol, which has already been described by Yoo et al. [7] and measured by Zhang et al. [13] by means of cyclic voltammetry. Also,

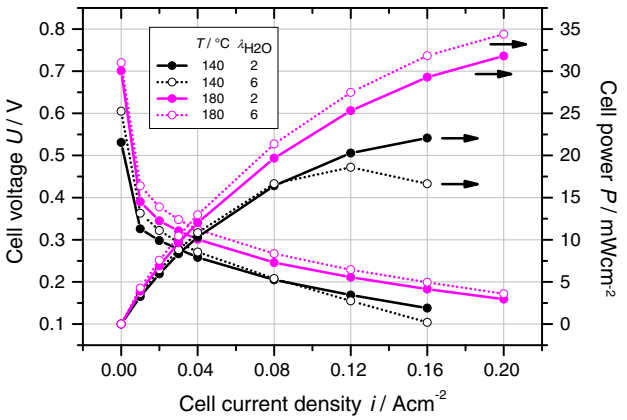

Fig. 1 Cell voltage and power versus cell current density with water stoichiometry λ_{H2O} as a parameter. λ_{H2O}, 2 and 6; λ_{DME}, 2; λ_{O2}, 3; cell temperature T, 140 and 180 °C; pressure, ambient atmosphere (~101 kPa); stoichiometric flow for current density $i > 0.04$ A cm^{-2}

Keranguévén et al. [12] assumed on the basis of IR reflectance measurements that adsorption of DME as part of the electro-oxidation takes place only at high potentials, leading to low cell voltages.

As expected, the performance is better at 180 °C than it is at 140 °C for water stoichiometries $\lambda_{H2O} = 2$ and 6. The increased temperature seems to improve the reaction kinetics. In previously proposed reaction pathways of DME at Pt, CO has always been assumed to be an intermediate species. Increasing the temperature leads to improved CO oxidation kinetics and thus to CO detoxification of the catalyst surface.

In addition, a higher water stoichiometry indicates a significant improvement in performance. The excess of water ensures that enough reactants are available to react with DME and its intermediates. According to Eqs. 2 and 3, water is necessary for the presumed electro-oxidation of Pt-bound CO [19]:

$$H_2O + 2(Pt) \rightleftharpoons OH(Pt) + H(Pt) \quad (2)$$

$$CO(Pt) + OH(Pt) \rightleftharpoons CO_2 + H(Pt) + (Pt) \quad (3)$$

Therefore, an increase in the amount of water can lead to elevated CO oxidation and thus to an increase in power. Elevated temperatures support this effect by facilitating the increased adsorption of OH which is the assumed species derived from the dissociation of water at Pt [17]. An additional positive effect could be enhanced proton conductivity. Theoretically, proton conductivity is independent of water content in a HT-PEM because conductivity is ensured instead by the phosphoric acid molecules. However, there is a dependence on relative humidity, as reported in [20]. As one can see in Fig. 2, the positive reaction order of water vapor is present only at low stoichiometries and saturates or even reverses for higher values of λ_{H2O}. The reason for this is that the displacement and dilution of DME by water is assumed.

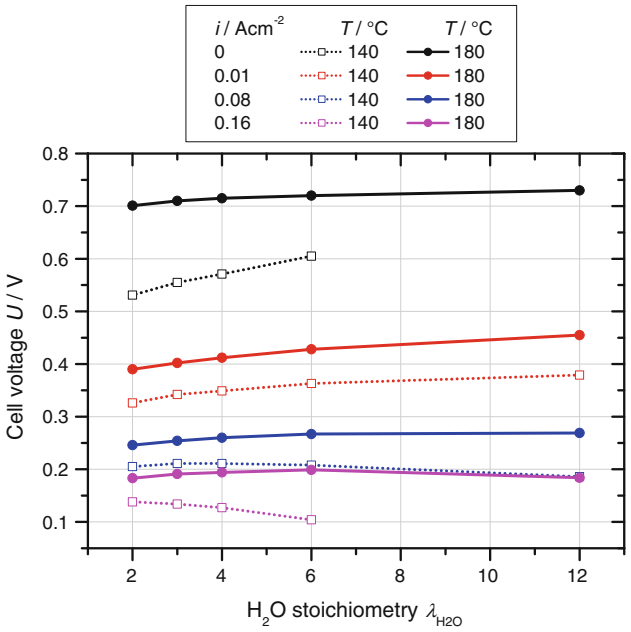

Fig. 2 Cell voltage versus water stoichiometry λ_{H2O} with cell current density i and cell temperature T as parameters. i 0, 0.01, 0.08, 0.16 A cm^{-2}; λ_{DME}, 2; λ_{O2}, 3; T, 140 and 180 °C; pressure, ambient atmosphere (~101 kPa); stoichiometric flow for $i > 0.04$ A cm^{-2}

At 180 °C and low cell current densities, one can see that a stoichiometry >6 leads to only slight further improvement, whereas at higher cell current densities the performance again decreases. At a cell temperature of 140 °C (open squares in Fig. 2), changes of voltage versus current density are even much more pronounced than they are at 180 °C. At low cell current densities, the cell power continuously increases with increasing water content, but under the same conditions, the power density decreases somewhat at higher cell current densities.

We were not able to perform measurements at even higher stoichiometries because the high humidity led to voltage fluctuations with peaks of up to 20 mV.

In Fig. 1, it can be seen that at a cell temperature of 140 °C, the curves of both investigated water stoichiometries intersect. This behavior is also observed at 160 and 170 °C, but the intersection is shifted toward higher cell current densities (not shown here). Therefore, it is expected that there is an intersection even at 180 °C, but it did so at a current density that could no longer be measured.

The observation that above a certain water vapor stoichiometry no further performance improvement can be seen and that actually a decrease in performance occurs indicates that the advantage of increasing the water content, i.e., better DME oxidation and detoxification, is being overridden by a dilution effect.

At maximum power at 180 °C in Fig. 1, the electrical efficiency is about 11 % according to the ratio of the

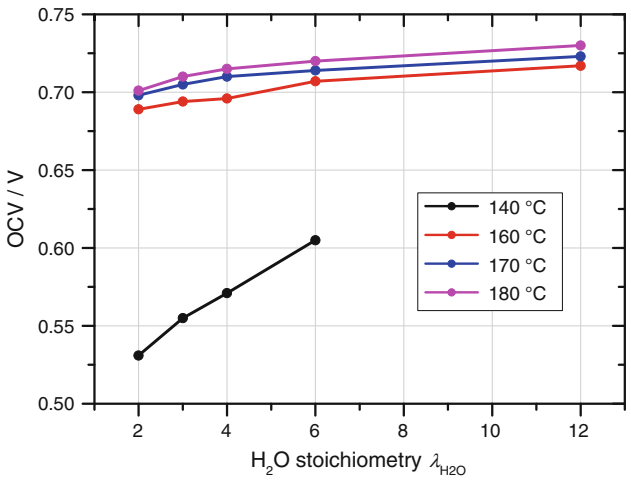

Fig. 3 OCV versus water stoichiometry with cell temperature T as a parameter. λ_{DME}, 2; λ_{O2}, 3; pressure, ambient atmosphere (~101 kPa)

respective voltage of 0.172 V and the thermoneutral voltage.

Figure 3 shows the open circuit voltage (OCV) versus water stoichiometry with cell temperature T as parameter. The OCV of DME (0.5–0.7 V) published by Haraguchi et al. [21] was confirmed by our measurements. Also, the fact that OCV increases with temperature, mentioned in [17], was observed. The OCV of DME cells are not determined by thermodynamics; instead, they mirror the change in the conversion rate of DME and the mixed potential formation at the cathode. Therefore, the low OCV even at 180 °C can be explained by the slow adsorption kinetics, as mentioned above, and the likelihood of a significant crossover of DME or an intermediate through the membrane, and thus of a high mixed potential. Figure 3 shows that the OCV increases slightly with increasing water stoichiometry. At temperatures above 160 °C, the curves show no significant difference. However, a pronounced difference can be seen at a cell temperature of 140 °C, indicating a high thermal activation. Here, the OCV increases strongly, but the voltage is significantly lower than that at higher temperatures. This clearly indicates the impact of temperature on the reaction kinetics of the internal reforming of DME.

For the following measurements, a water stoichiometry of 6 was selected unless otherwise indicated.

3.1.2 *Dependence on DME stoichiometry*

In terms of the variation of DME stoichiometry, there is an inverse behavior compared to that which occurs with water content. Figure 4 shows that the cell voltage decreases continuously with increasing DME stoichiometry at low temperatures and low cell current densities. With

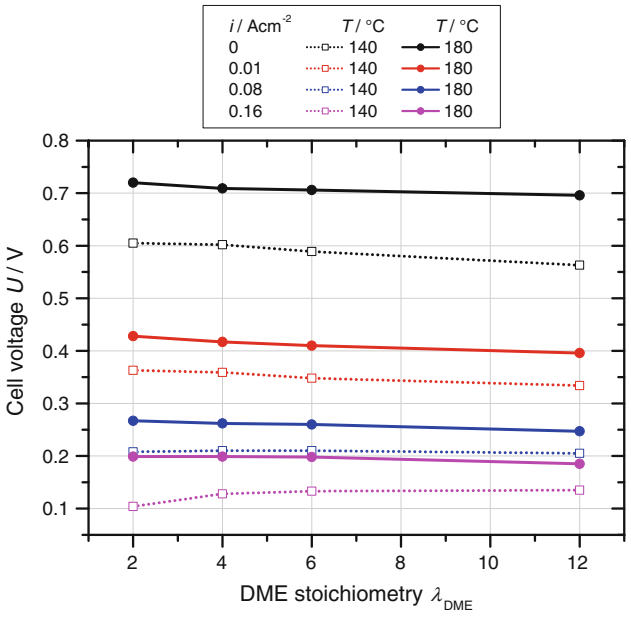

Fig. 4 Cell voltage versus DME stoichiometry λ_{DME} with cell current density i and cell temperature T as parameters. i 0, 0.01, 0.08, 0.16 A cm^{-2}; λ_{H2O}, 6; λ_{O2}, 3; T, 140 and 180 °C; pressure, ambient atmosphere (~101 kPa); stoichiometric flow for $i > 0.04$ A cm^{-2}

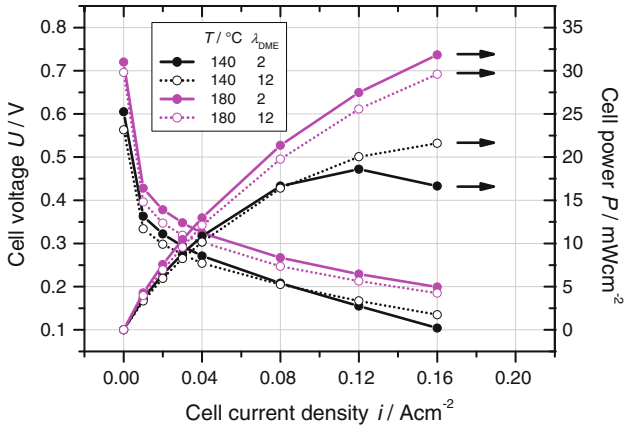

Fig. 5 Cell voltage and power versus cell current density with DME stoichiometry λ_{DME} as a parameter. λ_{DME}, 2 and 12; λ_{H2O}, 6; λ_{O2}, 3; cell temperature T, 140 and 180 °C; pressure, ambient atmosphere (~101 kPa); stoichiometric flow for current density $i > 0.04$ A cm^{-2}

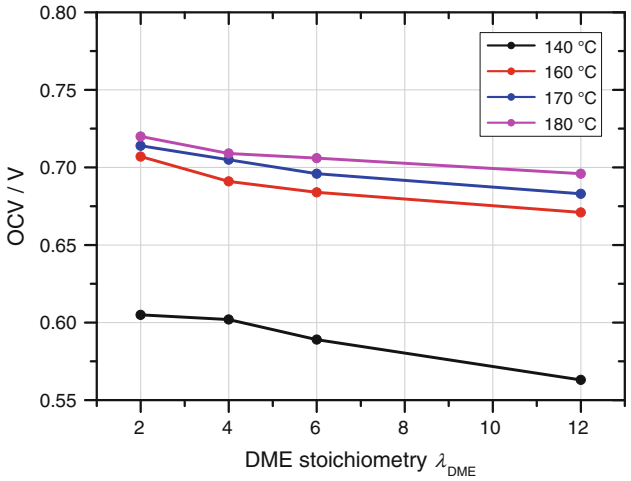

Fig. 6 OCV versus DME stoichiometry with cell temperature T as a parameter. λ_{H2O}, 6; λ_{O2}, 3; pressure, ambient atmosphere (~101 kPa)

increasing current density, this behavior reverses, i.e., the cell voltage increases with stoichiometry to an asymptotic value. At higher temperatures, there is only a decreasing trend of cell voltage for increasing stoichiometries at all investigated cell current densities.

The decreasing curve can be explained as resulting from CO poisoning caused by the relatively lower water content at the electrode or by the formation of a stronger mixed potential at the cathode with increasing DME stoichiometry. With increasing cell current, the higher overvoltage and thus higher CO oxidation rates counteracts the poisoning effect, so that the decrease attenuates or even reverses at lower temperatures. The increase at 140 °C and high current densities may possibly also indicate fuel depletion due to low DME flow.

Figure 5 shows the variation of cell voltage versus cell current density at the temperatures and stoichiometries corresponding to those in Fig. 4. At 180 °C, the curves are consistently above those at 140 °C, which in turn can be explained by the enhanced reaction kinetics. The explanation of the intersection of the two curves at 140 °C is consistent with the considerations which were made for Fig. 4. Due to the apparent behavior in further measurements, a DME stoichiometry of 2 was set except where indicated otherwise.

The trend of the OCV values with DME stoichiometry (Fig. 6) is consistent with previous results. The decrease is explained by decreased hydrogen production as a consequence of the decreasing water content in relation to DME. The significant decrease of OCV for the lowest measured temperature of 140 °C is striking and similarly observed in Fig. 3.

3.1.3 Gas chromatographic experiments

In addition to the $U(i)$ curves, the cathodic exhaust was analyzed by means of gas chromatography. Figures 7 and 8 show the CO_2 and O_2 concentrations versus cell current density with DME stoichiometry as a parameter.

It is noticeable that even in the currentless case, CO_2 is observed at the cathode, increasing with increasing DME flow. This indicates a participating diffusive effect that allows DME or a decomposition product to permeate through the membrane and to react to CO_2 at the cathode.

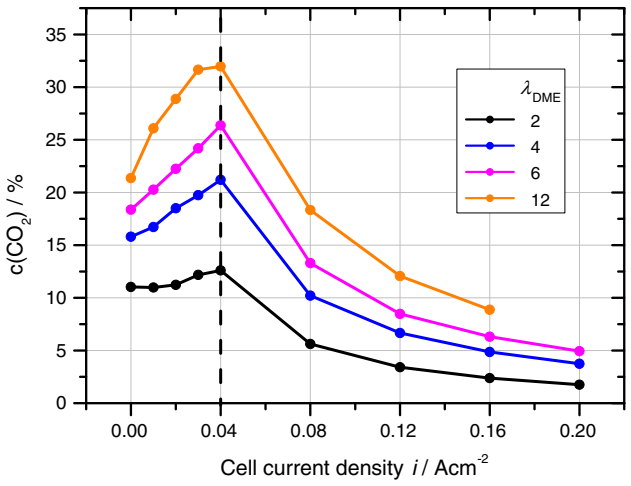

Fig. 7 CO_2 concentration in the cathode exhaust versus cell current density with DME stoichiometry as a parameter. λ_{H2O}, 6; λ_{O2}, 3; cell temperature T, 180 °C; pressure, ambient atmosphere (~101 kPa); stoichiometric flow for current density $i > 0.04$ A cm^{-2}

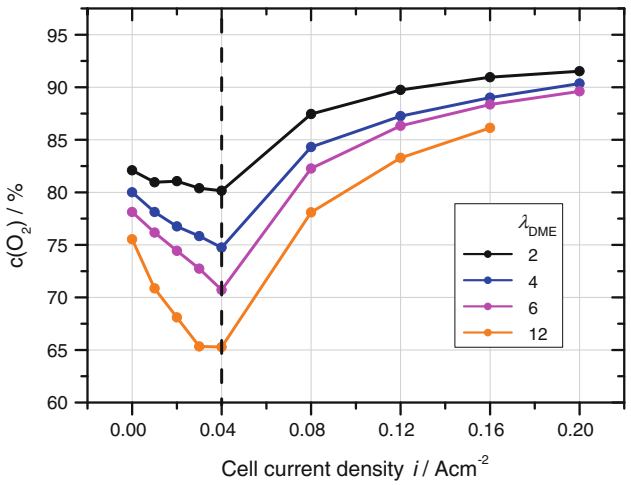

Fig. 8 O_2 concentration in the cathode exhaust versus cell current density with DME stoichiometry as a parameter. λ_{H2O}, 6; λ_{O2}, 3; cell temperature T, 180 °C; pressure, ambient atmosphere (~101 kPa); stoichiometric flow for current density $i > 0.04$ A cm^{-2}

This assumption is supported by the low open-cell voltages, which result from the formation of a mixed potential. Increasing the current density without changing the gas flow rates (0–0.04 A cm^{-2}) leads to a quasi-linear increase in CO_2 concentration and a linear decrease in O_2 concentration. The concentration of DME decreases slightly with increasing current density from 1.5 to 0.5 %. Even if the DME concentration decreases, the increase of CO_2 with increasing current density is the opposite of what occurs in a DMFC, where the crossover of methanol and, therefore, CO_2 production at the cathode monotonically decreases with increasing cell current. Similar behavior for DME is observed for the stoichiometric flow region from 0.04 to 0.2 A cm^{-2}, which can be interpreted similarly to the DMFC case.

In the low current regime with constant oxygen flow, there is a decreasing O_2 concentration at the cathode and a corresponding increase of CO_2. This indicates that the reaction to CO_2 takes place primarily at the cathode and that the increasing reaction rate at the anode does not significantly determine the DME anode concentration (note that the DME stoichiometry is very high). However, even small currents in the cell strongly influence the potential at the cathode (mixed potential formation from DME oxidation and oxygen reduction reaction) and lead to an increase of CO_2 and a decrease of O_2 formation. At currents higher than 0.04 A cm^{-2} the behavior reverses to that known from DMFCs.

However, the GC results were not specific enough to determine whether a DME or a decomposition product is crossing the membrane and which transfer process plays the most important role. With an increase of anodic water stoichiometry, the CO_2 concentration at the cathode strongly decreases (not shown here). One could assume increased CO_2 production already at the anode due to enhanced oxidation of DME intermediates. This behavior seems to indicate that CO_2 does not permeate the membrane significantly.

At a temperature of 140 °C, a qualitatively similar behavior emerges, with the difference that the CO_2 concentration is consistently lower and the O_2 concentration higher. This is due to the reduced reaction kinetics at lower temperatures. It is, however, conspicuous that the cathode DME concentration at 140 °C is up to ten times higher than at 180 °C. This is a qualitatively different behavior to that measured by Lobato et al. [9] with PBI-based DMFCs. He measured decreasing methanol permeation with increasing temperature. However, the detected behavior is still not well understood and further work is necessary to analyze CO_2 formation and transportation within the HT-PEFC

3.2 Dynamic operation

In order to determine if a cell can be used for a specific application, it is necessary to know the cell behavior during fast current transients. Unless otherwise specified, the measurements were performed with the following settings: pressure, ambient atmosphere (~101 kPa); DME flow, 19 ml min^{-1}; H_2O, 134 g min^{-1}; O_2, 84 ml min^{-1}. The flows correspond to the stoichiometries 2, 6, and 3 at a cell current density of 0.16 A cm^{-2}. After a change in cell current density, the new current density was maintained for 3 min to ensure the achievement of an equilibrium state.

Looking at the progression of the cell voltage immediately after a sudden change of load, several effects can be noticed (Fig. 9). After an increase of cell current, the

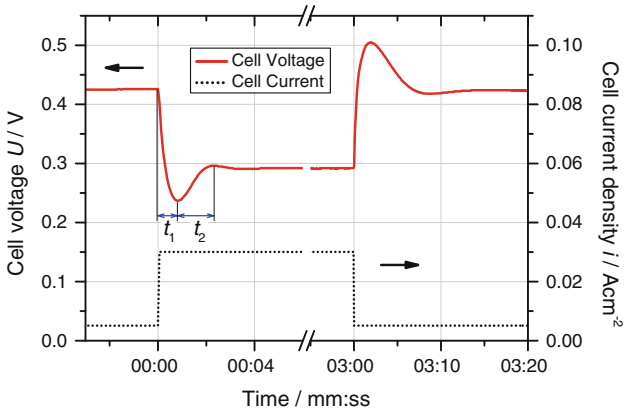

Fig. 9 Sketched temporal development of the cell voltage after a spontaneous positive and negative change of cell current density

voltage drops off sharply at first. It reaches a minimum after a time t_1 before increasing again. Sometimes one can see another much smaller maximum. Eventually, the voltage reaches steady state. This increase is characterized by the time t_2. After a sharp load step to lower values, a similar behavior with the opposite sign can be observed. In the range from microseconds to a few milliseconds after changing the cell current density, fast variations of the ohmic cell resistance and capacitive processes at the double-layer capacitance between electrolyte and electrode are responsible for the development of the cell voltage. In the further progression, electrochemical reaction rates increasingly play a role, which are dependent on the voltage between electrode and electrolyte. On a larger timescale, diffusive processes also occur. The latter two effects in particular are examined in more detail below.

As already mentioned, carbon monoxide is always a stable intermediate in the reaction of DME with water at the anode. Comparing the response of the cell voltage to spontaneous load cycles with a fuel cell, which operates with a H_2/CO mixture as fuel, one can clearly see qualitative similarities in the apparent over- and undershoots. Therefore, one can speculate that CO causes the same behavioral characteristics. In order to quantify the influence of the poisoning, the response of the cell voltage to various load changes was compared.

Figure 10 shows the cell voltage as a response to load changes of different amplitudes, starting from a common initial load. The reaction is shown for cell temperatures of 160 and 180 °C. With increasing amplitude of the cell current density, there is a clear decrease of t_1 and of the time required to reach the new steady state. At the same time, an increase in the amplitude of the undershoot is visible. At the beginning, before the load changes, all cell voltages, and hence the potential between electrode and electrolyte at the anode, are the same. Therefore, the surface coverage of the Pt catalyst is also the same. In the case of the largest amplitude of the current density change, there are, in comparison to the lower changes in amplitude, fewer free catalyst sites available. This explains the greater amplitude of the undershoot. At the same time, at higher cell current densities, the cell voltages decrease, which leads to enhanced CO oxidation and therefore to a decrease of t_2. In addition, t_1 also decreases with increasing load step amplitudes. These two effects, which were already suggested in [22] for a vapor-fed DMFC, cause a faster establishment of a new steady state for load changes with large amplitudes.

In Fig. 10a, the initial cell current density is 0 A cm^{-2}, and in Fig. 10b it is 0.02 A cm^{-2}. One can see that even with different initial cell current densities, the behavior is qualitatively similar. The differences, however, are much less pronounced in the latter case. Because the cell voltage already strongly drops at low current densities, the enhanced CO oxidation is responsible for the faster attainment of a steady state. The same applies to the comparison at the two temperatures of 160 and 180 °C. At the lower temperature, the effects are more pronounced, which can be attributed to reduced reaction kinetics. Because the differences are minor, however, one can assume that the occurrence of the undershoots is largely due to the varying oxidation kinetics of the Pt–CO compound at different overvoltages.

Figure 11 shows, based on the data from Fig. 10a and b, the progress of the times t_1 and t_2. Especially in the absence of an initial load, both times are high, which indicates a relatively high occupancy of the Pt sites. With increasing amplitude of load change, t_1 and t_2 are significantly reduced. Both times are also significantly reduced when the initial load is increased to only 0.02 A cm^{-2}. These results are due to the sharp drop in cell voltage even at low current densities and the consequently occurring enhanced oxidation. A change with further increases in the step current density is minimal.

A corresponding behavior of the cell voltages can be observed for changes to lower loads. Figure 12 shows load changes with three different amplitudes, each with the same step current density. It is clearly seen that the amplitude of the overshoot is smaller for the lower initial current densities. This trend can be understood when considering that in the case of small initial current densities, the CO poisoning is greater than it is in the case of high initial current densities in relation to the step current density, which is the same in all cases. Therefore, there are fewer free catalyst sites available at the final state of the cell. Because the step current density is the same in all cases, an identical defined CO oxidation occurs. Hence, for the case of the largest overshoot the time required to reach a steady state is the longest, whereas for the case of the smallest overshoot, the time is the shortest.

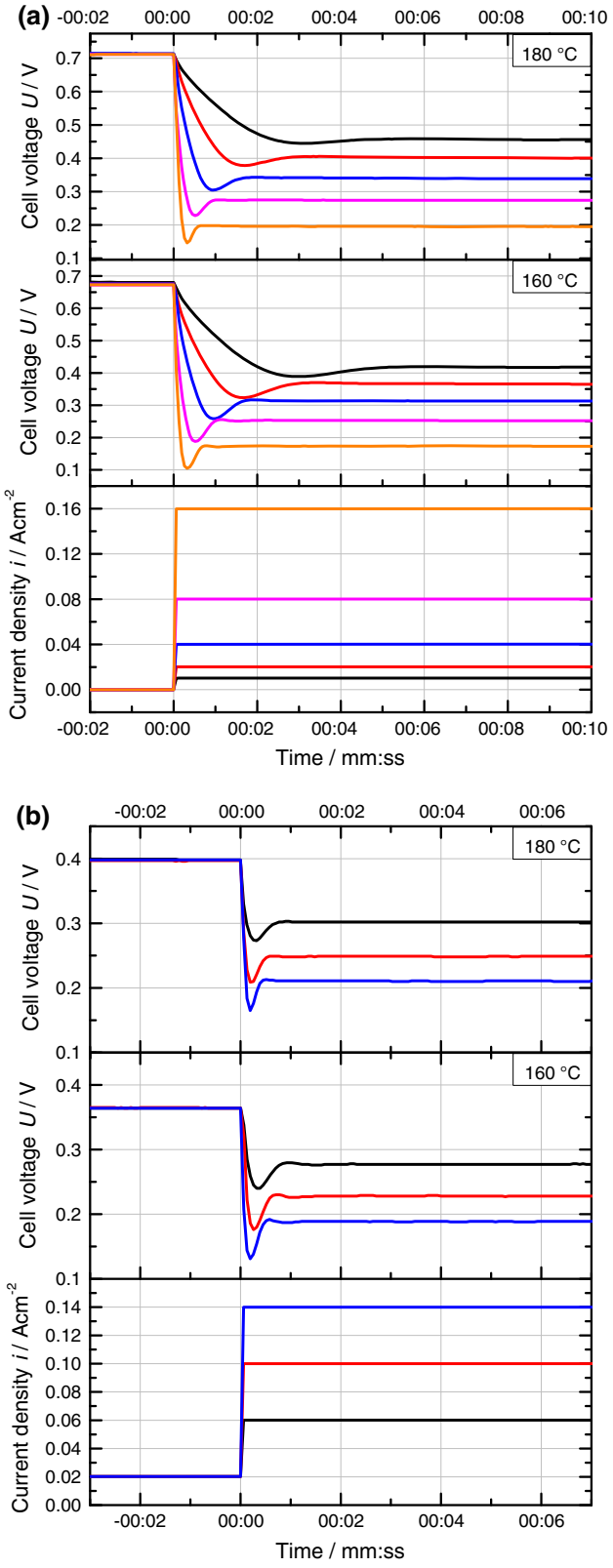

Fig. 10 Cell voltage after spontaneous positive changes of cell current density versus time at cell temperatures T of 160 and 180 °C. **a** Initial cell current density i, 0 A cm^{-2}. **b** Initial cell current density i, 0.02 A cm^{-2}

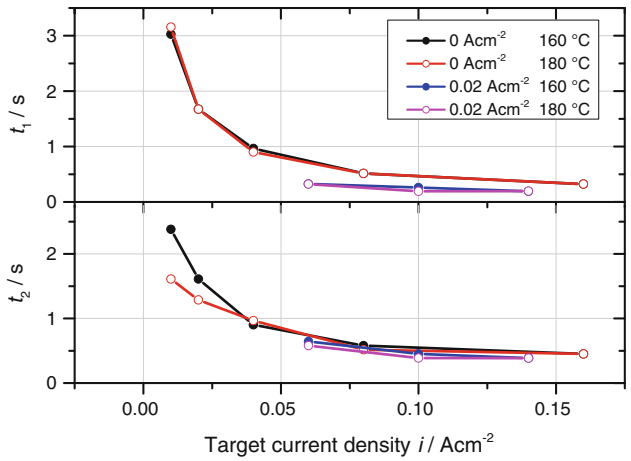

Fig. 11 Course of time t_1 and t_2 after a sudden load increase versus the step current density. Initial cell current densities i, 0 and 0.02 A cm^{-2}; cell temperatures T, 160 and 180 °C

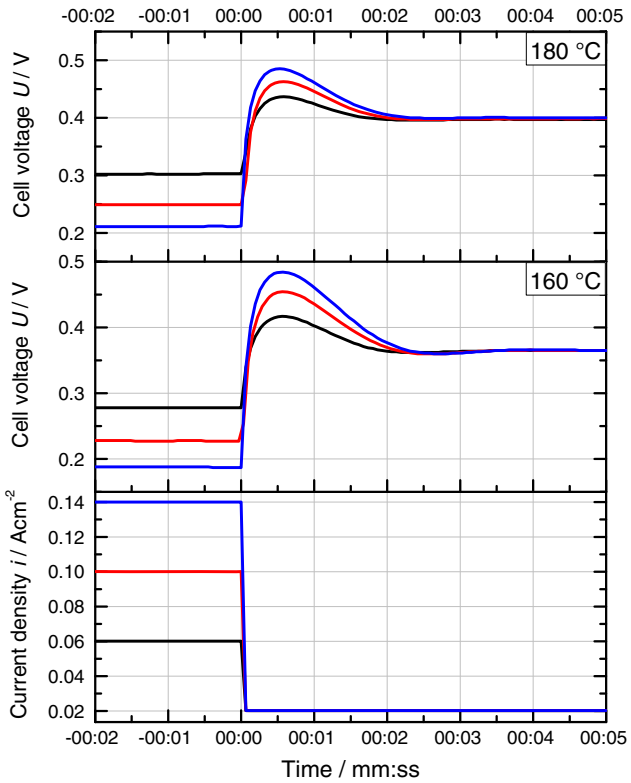

Fig. 12 Cell voltage after spontaneous negative changes of cell current density versus time at cell temperatures T of 160 and 180 °C. The step cell current density i is 0.02 A cm^{-2}

For a vapor-fed DMFC, Kallo [22] describes the cell voltage behavior after a spontaneous increase in load. They observe a continuous increase in cell voltage that takes place over several seconds. The reason for these results is that with increasing current density, permeation of methanol through the membrane decreases. This leads to a

lower mixed potential and hence a higher equilibrium cell voltage. In the case of DME as fuel, such an increase could not be observed at the low current side of the performance curve. As indicated by GC measurements, at low currents there is no decrease of mixed potential with increasing current density.

4 Conclusions

Promising experiments with methanol-fueled HT-PEFCs as well as their high CO tolerance motivated us to operate a PBI-based HT-PEFC with DME as the fuel. First, stationary measurements were performed at various temperatures and gas stoichiometries. As expected, enhanced power was achieved at cell temperatures of 180 °C compared to that at 160 °C, which can be attributed to improved reaction kinetics. Up to a stoichiometry of 6, the cell power improved with increasing water flow. This is explained by the greater availability of water as a reaction partner for DME and the availability of OH for the oxidation of Pt–CO bonds. With a higher water supply, the performance of the cell saturates and decreases slightly, which can be explained by a dilution of DME by the excess water. However, an increase of the DME stoichiometry has the opposite effect. In this case, the performance decreases with increasing flow, especially at high temperatures, in all examined areas of current density. This is caused by a relatively low supply of water, which is needed for the reaction.

There is a strong behavioral similarity to DMFCs, especially at the sharp drop of the cell voltage at low current densities in steady state. But even the dynamic behavior of the cell, examined in the second part of this work, shows similarities to DMFCs. After sudden changes of cell current density, the over- and undershoots that occurred were characterized and assigned to electrochemical effects, which consist primarily of a change of the CO oxidation rate.

In summary, one can say that the achieved power densities of 25 mW cm^{-2} and electrical efficiencies of about 11 % are not sufficient to realize fuel cell systems with HT-PEMs using DME as fuel. Therefore, improvements are necessary, both in terms of the materials used, especially the catalyst, and the optimization of the operating conditions.

Currently, the presented work is being continued. Due to degradation effects, an increase of operating temperature is not preferable. In the future, we plan to investigate both cell behavior when using alloy catalysts and the impact of phosphoric acid on catalyst poisoning.

Acknowledgments BASF kindly provided the Pt-based MEAs and a suitable cell holder.

References

1. Hogarth M, Christensen P, Hamnett A, Shukla A (1997) J Power Sources 69:125
2. Qi Z, Kaufman A (2002) J Power Sources 110:177
3. Good DA, Hanson J, Francisco JS, Li Z, Jeong GR (1999) J Phys Chem A103:10893
4. Semelsberger TA, Borup RL, Greene HL (2006) J Power Sources 156:497
5. Mench MM, Chance HM, Wang CY (2004) J Electrochem Soc 151(1):A144
6. Im JY, Kim BS, Choi HG, Cho SM (2008) J Power Sources 179:301
7. Yoo JH, Choi HG, Chung CH, Cho SM (2006) J Power Sources 163:103
8. Jensen JO (2011) International Patent WO 2011/035784
9. Lobato J, Can P, Rodrigo MA, Linares JJ, Linares J (2008) Energy Fuels 22:3335
10. Wang JT, Wainright JS, Savinell RF, Litt M (1996) J Appl Electrochem 26:751
11. Lin WF, Wang JT, Savinell RF (1997) J Electrochem Soc 144(6):1917
12. Kéranguéven G, Coutanceau C, Sibert E, Hahn F, Léger JM, Lamy C (2006) J Appl Electrochem 36:441
13. Zhang Q, Li Z, Wang S, Xing W, Yu R, Yu X (2008) Electrochim Acta 53:8298
14. Müller JT, Urban PM, Hölderich WF, Colbow KM, Zhang J, Wilkinson DP (2000) J Electrochem Soc 147(11):4058
15. Li Q, He R, Gao J-A, Jensen JO, Bjerrum NJ (2003) J Electrochem Soc 150(12):A1599
16. Das SK, Reis A, Berry KJ (2009) J Power Sources 193(2):691
17. Krishnan P, Park J-S, Kim C-S (2006) J Power Sources 159(2):817
18. Pan C, He R, Li Q, Jensen JO, Bjerrum NJ, Hjulmand HA, Jensen AB (2005) J Power Sources 145(2):392–398
19. Giorgi L, Pozio A, Bracchini C, Giorgi R, Turtù S (2001) J Appl Electrochem 31:325
20. Ma YL, Wainright JS, Litt MH, Savinell RF (2004) J Electrochem Soc 151(1):A8
21. Haraguchi T, Tsutsumi Y, Takagi H, Tamegai N, Yamashita S (2005) Electr Eng Jpn 150(3):19
22. Kallo J (2003) PhD Dissertation, Ulm (Germany)